CrossMark

VASCULAR BIOLOGY (J. HAMILTON, SECTION EDITOR)

PET Imaging of Atherosclerotic Disease: Advancing Plaque Assessment from Anatomy to Pathophysiology

Nicholas R. Evans[1] · Jason M. Tarkin[2] · Mohammed M. Chowdhury[3] · Elizabeth A. Warburton[1] · James H. F. Rudd[2]

Abstract Atherosclerosis is a leading cause of morbidity and mortality. It is now widely recognized that the disease is more than simply a flow-limiting process and that the atheromatous plaque represents a nidus for inflammation with a consequent risk of plaque rupture and atherothrombosis, leading to myocardial infarction or stroke. However, widely used conventional clinical imaging techniques remain anatomically focused, assessing only the degree of arterial stenosis caused by plaques. Positron emission tomography (PET) has allowed the metabolic processes within the plaque to be detected and quantified directly. The increasing armory of radiotracers has facilitated the imaging of distinct metabolic aspects of atherogenesis and plaque destabilization, including macrophage-mediated inflammatory change, hypoxia, and microcalcification. This imaging modality has not only furthered our understanding of the disease process in vivo with new insights into mechanisms but has also been utilized as a non-invasive endpoint measure in the development of novel treatments for atherosclerotic disease. This review provides grounding in the principles of PET imaging of atherosclerosis, the radioligands in use and in development, its research and clinical applications, and future developments for the field.

Keywords Atherosclerosis · Positron emission tomography · Coronary artery disease · Carotid stenosis

Introduction

Atherosclerosis is a leading cause of morbidity and mortality in the Western world. It is a systemic inflammatory disease that develops over decades, through initial vascular endothelial dysfunction, circulating monocyte recruitment and accumulation, maturation into a necrotic core, atheroma plaque destabilization, and finally plaque rupture [1, 2]. Plaque rupture, and subsequent atherothrombosis, is the primary etiology for myocardial infarction, while large vessel (carotid) atherosclerosis accounts for around one third of ischemic stroke cases [3]. As a reflection of the systemic nature of atherosclerosis, concomitant disease in both coronary and carotid arteries is estimated to occur in 28–58 % of asymptomatic individuals [4–6].

A challenge facing the clinical management of atherosclerosis is differentiating between "stable" and "vulnerable" atherosclerotic plaques, those at risk of rupture and symptomatic atherothrombosis. In clinical practice, the most commonly used carotid imaging modalities are computed tomography (CT) angiography and Doppler ultrasound. In coronary artery disease, while invasive angiography remains the gold standard anatomical imaging technique, non-invasive modalities (CT angiography or perfusion) are increasingly being used for individuals with stable symptoms and low to moderate risk profiles. Within stroke care, medical versus surgical management of carotid atherosclerosis is determined by the degree of luminal stenosis on these investigations. However, this simple

This article is part of the Topical Collection on *Vascular Biology*

✉ Nicholas R. Evans
  ne214@cam.ac.uk

[1] Department of Clinical Neurosciences, University of Cambridge, Cambridge Biomedical Campus, Hills Road, Cambridge CB2 0QQ, UK

[2] Division of Cardiovascular Medicine, University of Cambridge, Cambridge Biomedical Campus, Cambridge CB2 0QQ, UK

[3] Division of Vascular and Endovascular Surgery, Cambridge University Hospitals NHS Foundation Trust, Cambridge Biomedical Campus, Cambridge CB2 0QQ, UK

anatomical criterion fails to consider other plaque characteristics associated with risk of rupture. By combining samples from the Oxford Plaque Study and the Athero-Express Study, Howard et al. analyzed a pooled sample of 1640 symptomatic plaques. From this pooled data, they showed that plaque thrombus, fibrous content, macrophage infiltration, high microvessel density, and overall plaque instability were each significantly associated with predicted stroke risk [7].

Non-stenotic carotid atheroma has been implicated as a cause of previously classified "cryptogenic" stroke, with non-stenotic plaques demonstrating high-risk morphological features (hemorrhage, thrombus, or fibrous cap rupture) having a higher association with ischemic stroke than those without high-risk features [8, 9]. Furthermore, intravascular imaging of coronary artery atherosclerosis has demonstrated that a significant atheroma burden with a high risk of subsequent cardiac events may be present in the absence of luminal stenosis due to outward artery remodeling [10–12]. Similar findings of high-risk plaques in the presence of non-obstructive lesions have been shown in humans with imaging of coronary remodeling using CT [13, 14].

These limitations of conventional anatomical imaging in the assessment of atherosclerosis have led to increased interest in non-invasive imaging methods to identify features of plaque vulnerability and disease activity. Positron emission tomography (PET) is one such imaging modality that can detect and quantify the pathophysiological processes associated with atherogenesis and subsequent plaque destabilization. PET imaging was originally developed in the mid-twentieth century and is now used routinely in oncological clinical care, though its use as a research tool to measure pathophysiological processes in atherosclerosis is more recent, beginning in 2002. These early atherosclerosis PET imaging studies showed proof of principle for identification of symptomatic carotid atheroma in human subjects, and subsequent animal and human studies provided histological validation. In the intervening 15 years, both animal and human studies have been instrumental in the understanding of the disease process through the development of new PET radiotracers.

Principles of PET/CT

The complex nature of atherogenesis provides a range of pathophysiological pathways that may be exploited as targets for imaging, many of which are amenable to PET. These targets include inflammation, through hypoxia and apoptosis, to microcalcification. PET utilizes positron-emitting radioligands that accumulate at these different biological processes of interest, their accrual within regions of interest (ROIs) resulting in a localized concentration of emitted positrons that quickly encounter electrons in neighboring tissues, leading to annihilation reactions. Such reactions result in the emission of gamma

photons that can be detected by scintillation detectors in the PET scanner. Regions of tracer uptake detected by PET must be co-registered with CT imaging (PET/CT) or magnetic resonance imaging (PET/MRI) to localize the pathophysiological processes to an anatomical location.

A major advantage of PET is its very high sensitivity, allowing picomolar tracer concentrations to be detected that can be used to quantify the biological processes of interest. The most appropriate method for measuring radiotracer activity in vascular tissue remains a subject of debate and is discussed in later sections. The conventional measurement methods are the standardized uptake value (SUV) and tissue to background ratio (TBR). SUV represents the ratio of radiotracer concentration in the target tissue to the injected radiotracer activity adjusted for weight. SUV may be further analyzed as SUV_{max} and SUV_{mean}. The SUV_{max} is calculated using the highest tissue radiotracer concentration in the ROI, while SUV_{mean} is calculated using the mean tissue radiotracer concentration within the whole ROI. In contrast, TBR was devised to correct for blood uptake of radiotracer, the "blood pooling" effect. TBR is calculated as the ratio of the SUV of the arterial wall to the SUV in the mid-lumen of a large vein with no evident spill-over effect from neighboring tissues [15].

PET Radioligands

Specific radioligands can be used in PET imaging to target the metabolic processes involved in atherogenesis and plaque disruption. Broadly, the main pathophysiological processes associated with plaque vulnerability can be split into (i) inflammation (with radioligands targeting macrophages, including ^{18}F-fluorodeoxyglucose, somatostatin receptor ligands, and translocator protein ligands), (ii) microcalcification (^{18}F-sodium fluoride), and (iii) hypoxia (^{18}F-fluoromisonidazole).

While the technique is non-invasive, exposure to both the radiotracer and CT scan involves ionizing radiation. A 250 MBq dose of ^{18}F-fluorodeoxyglucose involves a radiation exposure of 5 mSv, in addition to the 0.45 mSv from the CT scan required for attenuation correction. Radiotracers themselves have been shown to have an excellent safety profile, with a review of 81,801 radiopharmaceutical doses showing no recorded adverse reactions [16].

^{18}F-Fluorodeoxyglucose

^{18}F-fluorodeoxyglucose (FDG) is the mainstay radioligand in PET imaging and consequently has been the most common radioligand used in imaging studies of atherosclerosis. Originally used for malignancy staging, incidental findings of FDG accumulation in arterial territories during whole-body scans heralded its utility for detecting and quantifying inflammation within atheroma [17]. FDG, a radionucleotide

analog of glucose, accumulates intracellularly in proportion to cellular demand for glucose. It is taken up into cells via facilitated glucose transporter member (GLUT) 1 and 3, which are upregulated during atherogenesis due to hypoxia within the atheroma core and once inside the cytoplasm undergoes phosphorylation by hexokinase to become ^{18}F-FDG-6-phosphate. ^{18}F-FDG-6-phosphate lacks a 2′ hydroxyl group and consequently is unable to enter the Krebs cycle and undergo glycolysis, subsequently diffusing slowly out of the cell. This resulting accumulation is readily quantifiable and can be used as a sensitive measure of metabolic activity, particularly given its very high signal-to-noise ratios in tissues without high metabolic activity (such as normal vessel wall and blood). The high concentration of proinflammatory macrophages in the vulnerable plaque provides such a tissue with a high metabolic activity (Fig. 1).

FDG-PET's ability to measure plaque inflammation non-invasively in a symptomatic population was demonstrated in early work by Rudd et al. where FDG uptake differentiated between symptomatic and asymptomatic carotid atheroma in human subjects [18], a finding that has been corroborated in recent larger studies [19•]. This increased uptake of FDG detected by PET/CT has been shown to correlate with histological macrophage density in animal models [20, 21] and excised atheroma following carotid endarterectomy [15, 22].

FDG uptake has been shown to identify symptomatic carotid plaques that were non-stenotic on high-resolution MRI, supporting the concept that the severity of stenosis is not the sole determinant for symptomatic plaque rupture [23]. However, this small study contrasted with another small pilot study that showed that although FDG uptake was higher in symptomatic arteries, uptake also correlated with the degree of stenosis [24]. In a large FDG-PET study by Tahara et al., only 29 % of asymptomatic individuals with carotid atherosclerosis found on Doppler screening had FDG uptake within the plaque, with no difference observed in the carotid intima-media thickness between inflamed and non-inflamed plaques [25]. The observed association between increased FDG uptake with high-risk morphological plaque features measured by CT reinforces this finding and the shortcomings of solely anatomical assessments of stenosis [26]. Multimodal imaging studies using FDG-PET and MRI have allowed comparison of tracer uptake with more accurate assessment of plaque morphological features. Silvera et al. imaged individuals with vascular risk factors and found FDG TBR_{mean} to be higher for lipid-rich plaques, which are often vulnerable to rupture, than for collagen-rich or calcified plaques with a lower risk of rupture [27].

In addition to its relation with the index plaque rupture, higher FDG uptake in carotid atheroma has been shown to be associated with a higher risk of recurrent cerebrovascular events, independent of the degree of luminal stenosis [28]. This is supported by an association of higher FDG uptake and microemboli detected by transcranial Doppler [29•].

FDG-PET techniques have helped elucidate the systemic nature of atherosclerosis (Fig. 2). FDG uptake correlates

Fig. 1 FDG-PET/CT showing high radiotracer uptake in the right common carotid artery (*arrow*)
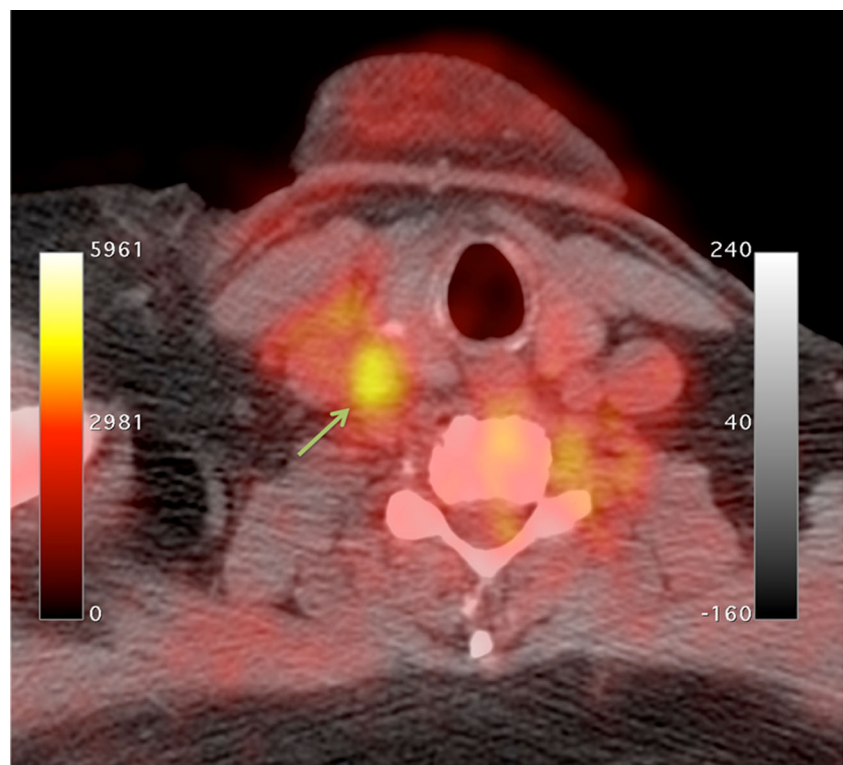
Fig. 2 FDG-PET/CT showing areas of focal radiotracer uptake in the wall of the descending aorta (*arrows*)
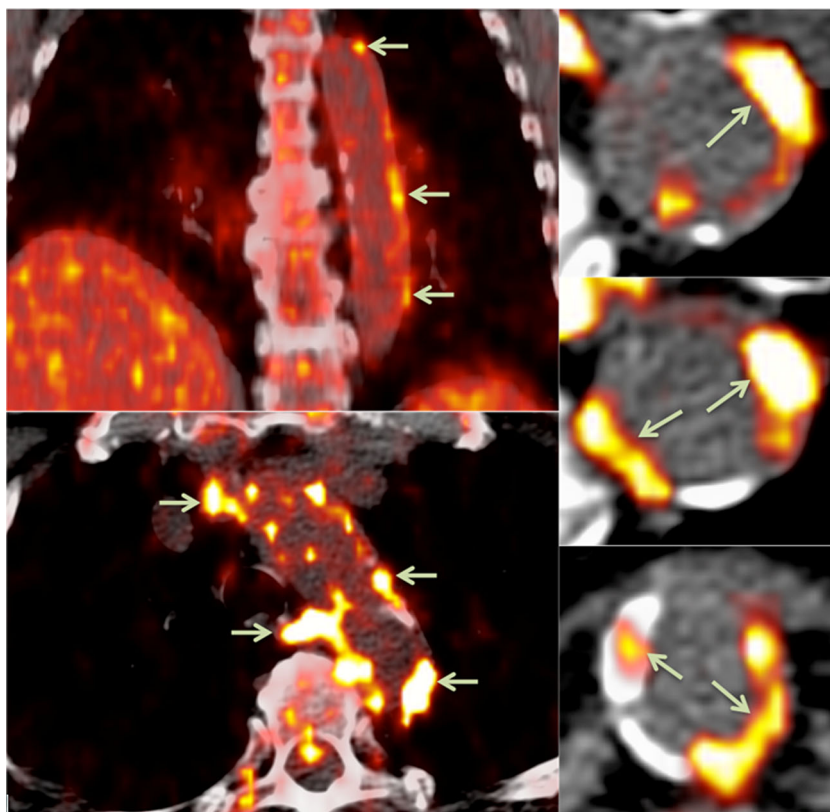
closely between neighboring arterial territories, suggesting a global upregulation of inflammation rather than a localized phenomenon [30••]. Joshi et al. demonstrated that FDG uptake in the aorta reflected the clinical severity of coronary syndromes, with a 20 % higher TBR in the aortas of those with a recent myocardial infarction than those with stable angina. Furthermore, within the group with myocardial infarcts, the aortic FDG uptake was higher for those with an ST elevation myocardial infarction than those with a non-ST elevation myocardial infarction [31]. Similarly, carotid SUV_{mean} and TBR_{mean} are significantly higher for cohorts with acute coronary syndrome than for those with chronic stable angina [32].

A possible mechanism for this relationship has been demonstrated through the association between focal arterial inflammation and systemic metabolic syndrome. Carotid TBR_{max} is higher in both non-obese individuals with metabolic syndrome and obese individuals without metabolic syndrome compared to non-obese individuals without metabolic syndrome [33]. Furthermore, both low-density lipoprotein and total cholesterol have been shown to be independently associated with FDG uptake [34, 35]. These findings go some way to explaining the association between higher Framingham risk factor scores and higher TBR.

The interface between systemic inflammation driving atheroma inflammation has been suggested by the association between periodontal inflammation and inflammatory activity

within atheroma, both of which reduced in response to atorvastatin and were strongly correlated [36, 37]. Serum inflammatory markers have been found to be associated with an increased risk of cardiovascular events, potentially representing either a cause or result of an upregulated inflammatory response [38–40]. Myeloperoxidase levels are associated with a higher FDG TBR in carotid diseased segments, independent of other conventional cardiovascular risk factors, although no independent relationship was found for high-sensitivity C-reactive protein (hsCRP), interleukin 6 (IL-6), or matrix-metalloproteinase 9 (MMP-9) [41]. However, other studies have provided conflicting results, with an association between higher TBR and higher levels of hsCRP [33, 42]. In comparison to blood biomarkers, FDG uptake can localize to focal sites of high inflammatory activity. The focal plaque inflammation on a background of a systemic inflammatory reaction may account for the finding of neighboring regions of FDG uptake.

Recent FDG-PET studies have continued to provide insights into the interactions and contributions of different aspects of the inflammatory process within atherosclerosis. In a prospective FDG-PET study, regions of the aorta with high SUV were more likely to develop calcification on subsequent CT imaging, independent of cardiovascular risk factors [43]. Furthermore, in a substudy of the dal-PLAQUE study, Joshi et al. found that FDG TBRs reduced over 6 months if carotid calcification was absent, though there was no interval change

in tracer uptake in carotid arteries where calcification was present [44]. Consequently, the authors concluded that calcium deposition is a propagating factor for ongoing arterial inflammation.

The accumulation of cholesterol crystals within atheroma has also been shown to promote plaque inflammation and rupture in animal models, while crystal content found in human carotid histology was found to be strongly associated with plaque disruption, thrombus, and symptoms [45–47]. Though there is no PET radioligand for imaging cholesterol crystals, instead relying on electron microscopy, their effect on inflammation within the plaque may be measured. Patel et al. showed that ezetimibe reduced the cholesterol crystal density on electron microscopy in the aortas of atherosclerotic rabbits, with a corresponding decrease in inflammation as quantified by FDG uptake (SUV_{max}), CRP, and MMP-9 levels [48].

FDG-PET has a number of advantages, but also limitations, compared to other imaging modalities. It is highly reproducible with high intra-observer and inter-observer agreement [49]. PET/CT using FDG has a high sensitivity for detecting inflammation in plaques, but its utility to detect inflammation may be hindered when the ROI is in close proximity to other tissues with tracer uptake due to high resting metabolic rates (such as neurons and myocardial tissue) and may be further compounded by the low spatial resolution of PET (approximately 3 mm). Solutions for both of these weaknesses are currently being developed with the advent of more cell-specific ligands and PET/MRI. Dynamic contrast enhanced (DCE) MRI has been shown to have superior spatial resolution than PET/CT, and contrast enhancement has been particularly effective in the assessment of fibrous cap thickness and lipid core volume, where the former enhances while the latter fails to enhance [50]. Multicontrast-weighted MRI has been used in surveillance of asymptomatic plaques and demonstrated larger lipid cores, thicker MWT, thin/ruptured fibrous caps, and intraplaque hemorrhage to each have significantly increased hazard ratios for subsequent symptomatic events [51]. However, while MRI offers an effective method for imaging morphological features associated with plaque vulnerability, it remains dependent on accurate coil placement as well as the reproducibility of technical sequences and image generation. These considerations, along with a desire to image directly the biological activity in the plaque, has led to DCE MRI and PET/CT providing complementary imaging of the plaque, though the advent of PET/MRI may enable a fusion of these techniques and is discussed further below.

Translocator Protein Ligands

While FDG-PET has become a mainstay of metabolic imaging in atherosclerosis in a relatively short time, its lack of specificity means that proximity of the artery of interest to other highly metabolically active structures, such as the myocardium, limits its utility. Alternative radiotracers targeting macrophage-driven inflammation via their expression of translocator protein (TSPO) have been investigated with the goal of providing higher specificity than that offered by FDG. ^{11}C-PK11195 (^{11}C-N-methyl-N-[1-methylpropyl]-1-[2-chlorophenyl]-isoquinoline-3-carboxamide) targets TSPO expressed on macrophages and microglia and has been shown to detect these inflammatory cells in atheroma and around the stroke penumbra, respectively. Specific to atherosclerosis, ^{11}C-PK11195 uptake was found to be higher in inflamed than non-inflamed plaques in a mouse model, though its utility as a tracer was limited due to a non-significant difference between plaque and healthy vessel wall [52]. This likely reflects the ubiquitous nature of TSPO expression by a range of cells and organs, despite the upregulation in activated plaque macrophages, but may also reflect the limitations of using mouse models of plaque, especially vulnerable plaques, compared to humans. Subsequent studies in human subjects have shown more promise, with ^{11}C-PK11195 TBR found to be higher in symptomatic versus asymptomatic carotid arteries (TBR 1.06 ± 0.2 and 0.86 ± 0.11, respectively, $p = 0.001$) despite a lower grade of stenosis in asymptomatic arteries [53]. ^{11}C-PK11195 uptake has been found to colocalize with activated macrophages using autoradiography and CD68 staining of ex vivo carotid histology [54, 55]. However, the ubiquitous uptake in healthy vessel wall may limit the utility of ^{11}C-PK11195-PET in clinical atherosclerosis imaging.

Newer TSPO ligands are in development, labeled with ^{18}F rather than [11]C. There has been increasing interest in ^{18}F-GE-180 (S-N,N-diethyl-9-[2-^{18}F-fluoroethyl]-5-methoxy 2,3,4,9-tetrahydro-1H-carbamazole-4-carboxamide) to replace PK-11195 as the TPSO ligand of choice to image neuroinflammation and potentially atherosclerotic plaque inflammation. Animal models have shown ^{18}F-GE-180 to have a significantly higher binding potential than that of PK-11195, improved signal-to-noise ratio, and lower non-specific binding in and around infarcted cerebral tissue [56, 57]. The use of ^{18}F in contrast to ^{11}C has other benefits including a longer half-life. However, the utility of such second-generation TSPO radioligands in PET imaging may be limited owing to variable receptor binding affinity due to genetic polymorphisms [58–60]. Further work is required to assess the utility of ^{18}F-GE-180 and other second-generation TSPO ligands for imaging both plaque inflammation and neuroinflammation.

^{68}Ga-DOTATATE and ^{64}Cu-DOTATATE

Another clinically available PET radioligand under investigation for use in atherosclerosis imaging is DOTATATE ([1,4,7,10-tetraazacyclododecane-N,N',N'',N'''-tetraacetic acid]-d-Phe1,Tyr3-octrotate). DOTATATE binds to somatostatin receptor subtype-2 (SST_2), which appears to be upregulated

on the surface of activated macrophages [61, 62]. The low physiological expression of SST$_2$ by the myocardium suggests that this tracer may be advantageous for targeting disease in the coronary arteries.

Vascular ^{68}Ga-DOTATATE uptake has been imaged in asymptomatic individuals with cardiovascular risk factors and coronary calcification [63–65] and in aortic atherosclerotic plaques in a mouse model [66]. In a retrospective series of DOTATATE-PET imaging performed in oncological practice, Rominger et al. found ^{68}Ga-DOTATATE-PET to have an excellent intra-reader and inter-reader reproducibility for TBR readings in the left anterior descending coronary artery (intra-class correlation coefficients of 0.97 and 0.94, respectively) [65].

[64]Cu-DOTATATE has also been investigated for use in carotid imaging. The longer half-life of ^{64}Cu compared to [68]Ga (12.7 h versus 68 min) and shorter maximum positron range provide several theoretical advantages, although this must be balanced against the wider availability of the generator-produced ^{68}Ga compared to the cyclotron-produced [64]Cu. In a proof-of-principle study using PET/MRI, Pedersen et al. demonstrated carotid ^{64}Cu-DOTATATE uptake correlated with gene expression of macrophage markers CD68 and CD163 using univariable analysis, though only correlation with CD163 expression remained significant on multivariable analysis [67]. DOTATATE's propensity toward CD163+ macrophages, as well as findings of atheromatous regions with DOTATATE but no FDG uptake, suggests that DOTATATE is able to identify a different component of the inflammatory process compared to conventional FDG-PET [65, 67]. Increased ^{64}Cu-DOTATATE signal has also been reported in individuals with cardiovascular risk factors in a retrospective study [68].

Although DOTATATE-PET has shown early promise as a potential candidate radiotracer for imaging inflammation in atherosclerosis, this newer technique has not yet been tested in large human studies in individuals with symptomatic disease. Further prospective clinical studies and histological validation are needed.

[18]F-Sodium Fluoride

Inflammation is not the sole metabolic process contributing to plaque vulnerability. Inflammation within the atheroma can promote microcalcification, the formation of deposits of calcium smaller than 50 μm, through cytokine-mediated promotion of osteoblast-like cells derived from vascular smooth muscle cells [69–71]. Plaque macrophage burden showed a strong association with osteoblastic activity in the aortas of hyperlipidemic mice, and both macrophage burden and osteogenic activity increased with plaque progression [72]. Microcalcification may predispose to plaque rupture either through mechanical disruption to the fibrous cap and/or provoking ongoing inflammation around the deposit.

[18]F-sodium fluoride (NaF) used in PET imaging is able to identify areas of microcalcification in vivo because the radiolabeled fluoride is taken up at sites of mineralization, where it replaces the hydroxyl group of hydroxylapatite [73] (Fig. 3). Work by Irkle et al. validated clinical NaF-PET using NaF against electron microscopy, autoradiography, and microPET for detecting microcalcification in symptomatic carotid endarterectomy histological specimens. Fluoride was shown to co-localize closely and preferentially bind to pathological mineralization, and the increased surface area of microcalcification relative to macrocalcification resulted in increased tracer uptake [74••].

The feasibility of NaF-PET to identify microcalcification in atherosclerotic plaques was demonstrated by Derlin et al. in a cohort of patients undergoing full-body NaF-PET/CT for oncological staging of bone metastases. This study showed that NaF uptake may occur at sites of macrocalcification, but distinct areas of NaF uptake and macrocalcification occurring in isolation demonstrated that NaF uptake reflects the active mineralization process in microcalcification rather than simply the burden of macrocalcification [75]. Further lack of co-localization between regional macrocalcification and regional NaF uptake has been found in other asymptomatic cohorts, with an inverse relationship between NaF uptake and plaque calcium score [76, 77]. Morbelli et al. demonstrate that the presence of cardiovascular risk factors correlate with NaF uptake but not arterial macrocalcification, though the study's measurement of uptake across the whole vessel may miss focal concomitant areas of macrocalcification and NaF uptake [76]. Further studies have found that carotid NaF uptake correlated with the presence of cardiovascular risk factors in an asymptomatic population [78]. Derlin et al. performed a dual-tracer PET/CT study using FDG-PET and NaF-PET in a further asymptomatic oncological patient cohort and found that of 215 arterial lesions identified by either tracer, only in 14 (6.5 %) was there concomitant FDG and NaF uptake, implying that macrophage-driven inflammation and microcalcification are two related but distinct processes [79].

A prospective study has shown that NaF TBR$_{max}$ is higher in individuals with coronary artery disease, stable angina, or previous cardiovascular events [80]. Increased tracer uptake has been shown to be associated with symptomatic coronary plaques, with the increased uptake seen in morphologically high risk but unruptured plaques suggesting that uptake reflects the microcalcification process rather than increased surface area following plaque rupture [81••]. In contrast, no significant difference in NaF uptake between symptomatic and asymptomatic carotids was found in a cohort of stroke patients, though the number of patients was small with long bolus to scan times [82].

The inter-rater repeatability of NaF-PET/CT is high, with an intra-class coefficient of 0.99 found in one study [80]. Further improvements in the quantification of microcalcification in coronary atherosclerosis is likely following developments in motion correction resulting in an improved signal-to-noise ratio,

Fig. 3 Lower limb ^{18}F-NaF imaging: non-contrast CT (*top left*) with a rim of calcification of the vessel, ^{18}F-NaF PET (*top right*), and fused ^{18}F-NaF PET/ CT (*bottom left*) of the superficial femoral artery (*arrow*) at the level of the adductor canal, demonstrating significant vessel uptake in this symptomatic patient. In addition, there is prominent uptake seen in the vessel at the same level on the coronal image (*bottom right*)
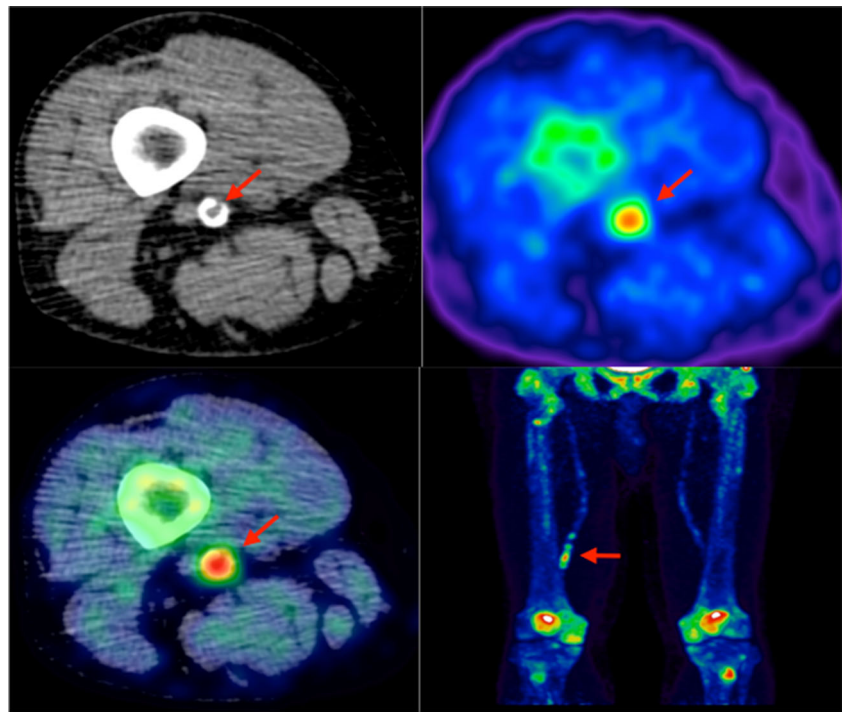
reducing signal "spill-over" from motion causing the radiotracer signal (detected over minutes) to fall outside the ROI determined from anatomical scans (taken over seconds) [83].

Quantifying Hypoxia

Atherosclerosis is often associated with hypoxia, presumably due to an increasing oxygen demand from foam cells. This likely results from reduced diffusion efficiency from lumen to wall as plaque thickness increases [84, 85]. Hypoxia potentiates the inflammatory response via hypoxia-inducible factor-1α (HIF-1α) expressed by macrophages in the core, a response that may be further upregulated by the presence of oxidized low-density lipoprotein [86, 87]. Whereas structural imaging techniques can assess the size of the necrotic core of the plaque, PET imaging using ^{18}F-fluoromisonidazole (FMISO) can measure the effects of hypoxia within the core directly. In a hypoxic environment, the FMISO is reduced and, in the absence of reoxidation, remains bound intracellularly. Mateo et al. demonstrated that in a hyperlipidemic rabbit model, FMISO uptake was significantly higher in regions of atheroma than in normal tissue. Furthermore, immunohistochemistry showed the hypoxia to be deep in the core rather than at the luminal boundary [88]. In an early clinical study, FMISO TBR was found to be higher in symptomatic than asymptomatic carotid atherosclerosis, with FMISO uptake correlating with FDG uptake, suggesting that hypoxia is a contributing factor in FDG uptake [89].

Recently, another radioligand targeting plaque hypoxia, ^{18}F-HX4 (^{18}F-2-(4-((2-nitro-1H-imidazol-1-yl)methyl)-1H-1,2,3-

triazol-1-yl)propan-1-ol), has been shown to have specific uptake in regions of plaque with a strong correlation between TBR$_{max}$ and carotid arterial wall dimensions on 3.0-T MRI [90].

Methodological Considerations

There are a number of methodological and technical considerations in PET/CT assessment of the plaque. At a single study level, these primarily include partial volume correction and methods of tracer uptake quantification. In contrast, the use of different study protocols within the field also has implications for reproducibility and the ability to pool results in larger meta-analyses.

Partial Volume Correction

Measurement of tracer uptake within the atheroma is dependent upon the size of the atheroma and the resolution of the scanner. The partial-volume effect occurs when limited resolution results in difficulty differentiating the tracer activity of the ROI from the tracer activity of the surrounding tissues. This may lead to "spill-out," where the tracer signal from the atheroma falls outside of the ROI, and "spill-in" where tracer signal from adjacent tissue falls within the ROI. The combination of these two effects results in partial volume error (PVE). Small atheromatous lesions falling below the spatial resolution of the scanner are particularly at risk of PVE. It is estimated that the dimensions of a homogenous ROI need to be two to three times the spatial resolution of the scanner in

order to minimize PVE [91]. Reduction of PVE through partial volume correction (PVC) can be performed using a geometric transfer matrix (GTM), whereby co-registration with a higher resolution modality allows restriction of the tracer signal to a corresponding voxel-based volume of interest that can then undergo further voxel-based adjustment for PVE using an algorithm proposed by Rousset el al. [92]. This method has been applied to atheroma imaging (using co-registration with MRI) and was found to improve quantification of tracer activity and to be highly reproducible [93].

SUV Versus TBR

Studies conducted to date have varied in their use of SUV or TBR, and the most appropriate quantification method remains a subject of debate [94]. In plaque simulations based on real patient data, marked bias was found in both measured SUV_{max} and SUV_{mean} compared to the modeled values, largely due to the spatial resolution of the reconstructed image typically being more than three times the thickness of the atherosclerotic plaque, resulting in a reduced ability to correct for PVE. Bias was more marked when fewer iterations were used during image reconstruction [94].

In a study of 32 patients undergoing endarterectomy, Niccoli et al. compared the ability of SUV_{max}, SUV_{mean}, TBR_{max}, and TBR_{mean} to differentiate in vivo plaques classified as either inflamed or non-inflamed following histological examination ex vivo. Within the symptomatic arteries, the authors found that the differences for SUV_{max} and SUV_{mean} between inflamed and non-inflamed plaques were non-significant, while both TBR_{max} and TBR_{mean} were able to differentiate between plaques found to be inflamed or non-inflamed on histology [95].

TBR has limitations, and its application is not without its criticisms. Blood-pool SUV has been shown to decrease with increasing injection to scan intervals (mean SUV within the jugular vein was 1.04 ± 0.16 at 1 h, 0.79 ± 0.03 at 2 h, 0.66 ± 0.04 at 3 h). Consequently, plaque TBR values differed significantly between cohorts scanned at 2 and 3 h. In contrast, tissue SUV_{max} did not differ between these time points [96]. Furthermore, impaired renal function will also contribute to increased blood-pool activity. Blood-pool SUV has been found to be inversely proportional to the estimated glomerular filtration rate, resulting in a lower TBR with lower renal clearance [97].

There has been an overall shift toward TBR in arterial PET imaging, but the possible confounders described above must be considered when comparing results both within the same study and against other studies. Standardization of scan methodologies and patient cohorts will help address this.

Reproducibility

Increasingly, specific radioligands have resulted in improved signal-to-background ratios and reproducibility, with high intra-rater and inter-rater reproducibility reported for NaF

and ^{68}Ga-DOTATATE [65, 80]. However, a major consideration within the field of vascular PET imaging is the wider reproducibility of individual studies. Typically, most vascular PET studies of symptomatic patients are small, with fewer than 50 participants, due to a combination of sufficient statistical power with small participant numbers balanced against radiation exposure and high economic costs. While the multitude of FDG studies would seem prime for meta-analysis, the heterogeneous patient populations and variations in methodology pose barriers to such analyses. Variations in tracer doses, interval between symptoms and imaging, blood glucose thresholds, and measurement techniques (SUV versus TBR) are a few of the differences in studies that make direct comparison difficult. The effect of the symptom to scan interval on the potential variability of the PET signal is difficult to quantify as radiation exposure is a barrier to longitudinal studies and should therefore be analyzed in any multivariate analysis. Consequently, there is a move toward establishing a recognized common standard for arterial PET imaging. A recent position paper from the European Association of Nuclear Medicine has recommended such common standards for FDG-PET, particularly with regards to injected dose, circulation uptake time, prescan fasting glucose limits, and suggested quantification using TBR in most cases [98]. Adopting a unified approach to scanning protocols and quantification will allow the high inter-rater reproducibility to be exploited, existing data to be pooled into larger meta-analyses, and standardization of multicenter PET imaging studies.

PET/CT Applications in Atherosclerosis Drug Trials

As well as its utility for understanding the pathophysiology of atherosclerosis, PET/CT has an important application for measuring the effects of drug treatment. FDG-PET has also offered key insights into mechanisms of atheroma stabilization with statins, in particular their observed anti-inflammatory effects upon the atheroma in addition to their effect on lipid profiles [99–101].

The capacity to measure atherosclerotic metabolic processes non-invasively in vivo has been shown to provide a useful endpoint for drug discovery and efficacy trials. The dal-PLAQUE phase 2b randomized clinical trial of dalcetrapib (a modulator of cholesteryl ester transfer protein that raises high-density lipoprotein cholesterol) used FDG uptake as its primary endpoint and demonstrated that there was no safety concerns over the 6 months while on dalcetrapib. In this study, dalcetrapib failed to reduce carotid FDG uptake when compared to placebo, which was consistent with the later randomized placebo-controlled clinical outcome study [102, 103]. FDG-PET endpoints have also been used by Emami et al. who used it to compare the therapeutic effects of BMS-582949 (a p38 mitogen-activated protein kinase inhibitor)

against placebo, but again, no significant difference was seen between these two cohorts [104]. This study did reinforce the finding that statin treatment leads to a reduction in FDG uptake in the control group, and this may contribute to the lack of significance between cohorts. These studies serve as an important proof of principle for the use of PET endpoints in randomized clinical trials.

Future Directions

Recent advances have led to the feasibility of MRI for anatomical co-registration with PET. PET/MRI has a number of potential advantages over PET/CT. MRI, using either contrast enhancement or black-blood imaging, has proven to be an effective non-invasive imaging modality for assessing and quantifying plaque morphological features. The complementary nature of MRI and PET for assessing plaque morphology and metabolism, respectively, is advantageous in the identification of vulnerable plaques [27, 105, 106]. However, currently, this requires two different scans with consequent difficulties for co-registration. Recent small studies on hybrid PET/MRI scanners have shown promising proof-of-principle data for combined morphological and metabolic imaging of atherosclerosis. In an asymptomatic cohort, Ripa et al. found a moderate to good correlation for PET/CT and PET/MRI FDG SUV_{max} ($r=0.6$) and SUV_{mean} ($r=0.8$) on carotid vessel-by-vessel comparison, though there was noted a small but significant under-reading for PET/MRI of less than -0.2 for both SUV_{max} and SUV_{mean} [107]. Hyafil et al. performed FDG-PET/MRI in a cohort of 18 cryptogenic strokes for individuals with "non-stenosing" carotid disease (i.e., stenosis measured as ≤50 %) and found that there was a significantly higher proportion of plaques with the highest morphological features of vulnerability (AHA lesion type 6, so-called complicated plaques) in the ipsilateral carotid compared to the side contralateral to the infarct. The FDG TBR_{mean} of both the ipsilateral and contralateral carotid arteries of individuals found to have AHA type 6 lesions was higher than the TBR_{mean} of individuals without complicated carotid disease [108]. Additional larger studies are required to evaluate the utility of PET/MRI, in particular regarding considerations such as attenuation correction and the implications for PVE.

Conclusions

The evolution of atherosclerosis imaging from anatomical to metabolic imaging has provided novel insights into the pathophysiology underlying atherogenesis and plaque vulnerability. Broad adoption within routine clinical care is currently limited by availability, cost, and radiation exposure. However, as a research tool, it has facilitated the introduction

of metabolic endpoints in studies of new treatments for atherosclerosis, as well as a means to measure the therapeutic effects of existing treatments. Translation of PET/CT techniques such as these to the clinical setting will require phase 3 trials where treatment decisions are made on the basis of metabolic imaging data rather than conventional structural imaging. The potential for newer, more specific radioligands and the increasing availability of PET/MRI is likely to advance our understanding of atherosclerosis and help the development of novel therapeutics to combat this important disease.

Compliance with Ethical Standards

Human and Animal Rights and Informed Consent This article does not contain any studies with human or animal subjects performed by any of the authors.

References

Papers of particular interest, published recently, have been highlighted as:
• Of importance
•• Of major importance

1. Libby P, Tabas I, Fredman G, Fisher EA. Inflammation and its resolution as determinants of acute coronary syndromes. Circ Res. 2014;114(12):1867–79.
2. Hansson GK, Libby P, Tabas I. Inflammation and plaque vulnerability. J Intern Med. 2015;278(5):483–93.

3. Chung JW, Park SH, Kim N, et al. Trial of ORG 10172 in Acute Stroke Treatment (TOAST) classification and vascular territory of ischemic stroke lesions diagnosed by diffusion-weighted imaging. J Am Heart Assoc. 2014;3(4), e001119.

4. Baber U, Mehran R, Sartori S, et al. Prevalence, impact, and predictive value of detecting subclinical coronary and carotid atherosclerosis in asymptomatic adults: the BioImage study. J Am Coll Cardiol. 2015;65(11):1065–74.

5. Sillesen H, Muntendam P, Adourian A, et al. Carotid plaque burden as a measure of subclinical atherosclerosis: comparison with other tests for subclinical arterial disease in the High Risk Plaque BioImage study. JACC Cardiovasc Imaging. 2012;5(7):681–9.

6. Bjerrum IS, Sand NP, Poulsen MK, et al. Non-invasive assessments reveal that more than half of randomly selected middle-aged individuals have evidence of subclinical atherosclerosis: a DanRisk substudy. Int J Cardiovasc Imaging. 2013;29(2):301–8.

7. Howard DP, van Lammeren GW, Rothwell PM, et al. Symptomatic carotid atherosclerotic disease: correlations between plaque composition and ipsilateral stroke risk. Stroke. 2015;46(1):182–9.

8. Freilinger TM, Schindler A, Schmidt C, et al. Prevalence of nonstenosing, complicated atherosclerotic plaques in cryptogenic stroke. JACC Cardiovasc Imaging. 2012;5(4):397–405.

9. Gupta A, Gialdini G, Lerario MP, et al. Magnetic resonance angiography detection of abnormal carotid artery plaque in patients with cryptogenic stroke. J Am Heart Assoc. 2015;4(6), e002012.

10. Mann JM, Davies MJ. Vulnerable plaque. Relation of characteristics to degree of stenosis in human coronary arteries. Circulation. 1996;94(5):928–31.

11. Oemrawsingh RM, Cheng JM, Garcia-Garcia HM, et al. Near-infrared spectroscopy predicts cardiovascular outcome in patients with coronary artery disease. J Am Coll Cardiol. 2014;64(23): 2510–8.

12. Ota H, Magalhaes MA, Torguson R, et al. The influence of lipid-containing plaque composition assessed by near-infrared spectroscopy on coronary lesion remodelling. Eur Heart J Cardiovasc Imaging. 2015. doi:10.1093/ehjci/jev221.

13. Motoyama S, Ito H, Sarai M, et al. Plaque characterization by coronary computed tomography angiography and the likelihood of acute coronary events in mid-term follow-up. J Am Coll Cardiol. 2015;66(4):337–46.

14. Puchner SB, Liu T, Mayrhofer T, et al. High-risk plaque detected on coronary CT angiography predicts acute coronary syndromes independent of significant stenosis in acute chest pain: results from the ROMICAT-II trial. J Am Coll Cardiol. 2014;64(7):684–92.

15. Tawakol A, Migrino RQ, Bashian GG, et al. In vivo 18F-fluorodeoxyglucose positron emission tomography imaging provides a noninvasive measure of carotid plaque inflammation in patients. J Am Coll Cardiol. 2006;48(9):1818–24.

16. Silberstein EB. Prevalence of adverse reactions to positron emitting radiopharmaceuticals in nuclear medicine. Pharmacopeia Committee of the Society of Nuclear Medicine. J Nucl Med. 1998;39(12):2190–2.

17. Yun M, Yeh D, Araujo LI, Jang S, Newberg A, Alavi A. F-18 FDG uptake in the large arteries: a new observation. Clin Nucl Med. 2001;26(4):314–9.

18. Rudd JHF, Warburton EA, Fryer TD, et al. Imaging atherosclerotic plaque inflammation with [18F]-fluorodeoxyglucose positron emission tomography. Circulation. 2002;105(23):2708–11.

19.• Skagen K, Johnsrud K, Evensen K, et al. Carotid plaque inflammation assessed with (18)F-FDG PET/CT is higher in symptomatic compared with asymptomatic patients. Int J Stroke. 2015;10(5):730–6. **A recent large study demonstrating the utility of FDG-PET to differentiate between symptomatic and asymptomatic carotid atheroma**.

20. Hyafil F, Cornily JC, Rudd JH, Machac J, Feldman LJ, Fayad ZA. Quantification of inflammation within rabbit atherosclerotic plaques using the macrophage-specific CT contrast agent N1177: a comparison with 18F-FDG PET/CT and histology. J Nucl Med. 2009;50(6):959–65.

21. Davies JR, Izquierdo-Garcia D, Rudd JH, et al. FDG-PET can distinguish inflamed from non-inflamed plaque in an animal model of atherosclerosis. Int J Cardiovasc Imaging. 2010;26(1):41–8.

22. Liu J, Kerwin WS, Caldwell JH, et al. High resolution FDG-microPET of carotid atherosclerosis: plaque components underlying enhanced FDG uptake. Int J Cardiovasc Imaging. 2015. doi: 10.1007/s10554-015-0739-2.

23. Davies JR, Rudd JH, Fryer TD, et al. Identification of culprit lesions after transient ischemic attack by combined 18F fluorodeoxyglucose positron-emission tomography and high-resolution magnetic resonance imaging. Stroke. 2005;36(12): 2642–7.

24. Arauz A, Hoyos L, Zenteno M, Mendoza R, Alexanderson E. Carotid plaque inflammation detected by 18F-fluorodeoxyglucose-positron emission tomography. Pilot study. Clin Neurol Neurosurg. 2007;109(5):409–12.

25. Tahara N, Kai H, Nakaura H, et al. The prevalence of inflammation in carotid atherosclerosis: analysis with fluorodeoxyglucose-positron emission tomography. Eur Heart J. 2007;28(18):2243–8.

26. Figueroa AL, Subramanian SS, Cury RC, et al. Distribution of inflammation within carotid atherosclerotic plaques with high-risk morphological features: a comparison between positron emission tomography activity, plaque morphology, and histopathology. Circ Cardiovasc Imaging. 2012;5(1):69–77.

27. Silvera SS, Aidi HE, Rudd JH, et al. Multimodality imaging of atherosclerotic plaque activity and composition using FDG-PET/CT and MRI in carotid and femoral arteries. Atherosclerosis. 2009;207(1):139–43.

28. Marnane M, Merwick A, Sheehan OC, et al. Carotid plaque inflammation on 18F-fluorodeoxyglucose positron emission tomography predicts early stroke recurrence. Ann Neurol. 2012;71(5): 709–18.

29.• Moustafa RR, Izquierdo-Garcia D, Fryer TD, et al. Carotid plaque inflammation is associated with cerebral microembolism in patients with recent transient ischemic attack or stroke: a pilot study. Circ Cardiovasc Imaging. 2010;3(5):536–41. **Study demonstrates how inflammation as measured by FDG-PET is associated with plaque instability and microembolic events on transcranial Doppler**.

30.•• Rudd JH, Myers KS, Bansilal S, et al. Relationships among regional arterial inflammation, calcification, risk factors, and biomarkers: a prospective fluorodeoxyglucose positron-emission tomography/computed tomography imaging study. Circ Cardiovasc Imaging. 2009;2(2):107–15. **Study demonstrates the systemic nature of atheromatous inflammation as measured by FDG-PET**.

31. Joshi NV, Toor I, Shah AS, et al. Systemic atherosclerotic inflammation following acute myocardial infarction: myocardial infarction begets myocardial infarction. J Am Heart Assoc. 2015;4(9), e001956.

32. Kim S, Lee S, Kim JB, et al. Concurrent carotid inflammation in acute coronary syndrome as assessed by (18)F-FDG PET/CT: a possible mechanistic link for ischemic stroke. J Stroke Cerebrovasc Dis. 2015;24(11):2547–54.

33. Yoo HJ, Kim S, Hwang SY, et al. Vascular inflammation in metabolically abnormal but normal-weight and metabolically healthy obese individuals analyzed with (1)(8)F-fluorodeoxyglucose positron emission tomography. Am J Cardiol. 2015;115(4):523–8.

34. Chróinín DN, Marnane M, Akijian L, et al. Serum lipids associated with inflammation-related PET-FDG uptake in symptomatic carotid plaque. Neurology. 2014;82(19):1693–9.

35. Kaida H, Tahara N, Tahara A, et al. Positive correlation between malondialdehyde-modified low-density lipoprotein cholesterol

and vascular inflammation evaluated by 18F-FDG PET/CT. Atherosclerosis. 2014;237(2):404–9.

36. Tonetti MS, D'Aiuto F, Nibali L, et al. Treatment of periodontitis and endothelial function. N Engl J Med. 2007;356(9):911–20.

37. Subramanian S, Emami H, Vucic E, et al. High-dose atorvastatin reduces periodontal inflammation: a novel pleiotropic effect of statins. J Am Coll Cardiol. 2013;62(25):2382–91.

38. Danesh J, Wheeler JG, Hirschfield GM, et al. C-reactive protein and other circulating markers of inflammation in the prediction of coronary heart disease. N Engl J Med. 2004;350(14):1387–97.

39. Sarwar N, Butterworth AS, Freitag DF, et al. Interleukin-6 receptor pathways in coronary heart disease: a collaborative meta-analysis of 82 studies. Lancet. 2012;379(9822):1205–13.

40. Meuwese MC, Stroes ES, Hazen SL, et al. Serum myeloperoxidase levels are associated with the future risk of coronary artery disease in apparently healthy individuals: the EPIC-Norfolk Prospective Population Study. J Am Coll Cardiol. 2007;50(2):159–65.

41. Duivenvoorden R, Mani V, Woodward M, et al. Relationship of serum inflammatory biomarkers with plaque inflammation assessed by FDG PET/CT: the dal-PLAQUE study. JACC Cardiovasc Imaging. 2013;6(10):1087–94.

42. Yoo HJ, Kim S, Park MS, et al. Vascular inflammation stratified by C-reactive protein and low-density lipoprotein cholesterol levels: analysis with 18F-FDG PET. J Nucl Med. 2011;52(1):10–7.

43. Abdelbaky A, Corsini E, Figueroa AL, et al. Focal arterial inflammation precedes subsequent calcification in the same location: a longitudinal FDG-PET/CT study. Circ Cardiovasc Imaging. 2013;6(5):747–54.

44. Joshi FR, Rajani NK, Abt M, et al. Does vascular calcification accelerate inflammation?: a substudy of the dal-PLAQUE Trial. J Am Coll Cardiol. 2016;67(1):69–78.

45. Abela GS, Aziz K. Cholesterol crystals rupture biological membranes and human plaques during acute cardiovascular events—a novel insight into plaque rupture by scanning electron microscopy. Scanning. 2006;28(1):1–10.

46. Vedre A, Pathak DR, Crimp M, Lum C, Koochesfahani M, Abela GS. Physical factors that trigger cholesterol crystallization leading to plaque rupture. Atherosclerosis. 2009;203(1):89–96.

47. Abela GS, Aziz K, Vedre A, Pathak DR, Talbott JD, Dejong J. Effect of cholesterol crystals on plaques and intima in arteries of patients with acute coronary and cerebrovascular syndromes. Am J Cardiol. 2009;103(7):959–68.

48. Patel R, Janoudi A, Vedre A, et al. Plaque rupture and thrombosis are reduced by lowering cholesterol levels and crystallization with ezetimibe and are correlated with fluorodeoxyglucose positron emission tomography. Arterioscler Thromb Vasc Biol. 2011;31(9):2007–14.

49. Rudd JH, Myers KS, Bansilal S, et al. Atherosclerosis inflammation imaging with 18F-FDG PET: carotid, iliac, and femoral uptake reproducibility, quantification methods, and recommendations. J Nucl Med. 2008;49(6):871–8.

50. Cai J, Hatsukami TS, Ferguson MS, et al. In vivo quantitative measurement of intact fibrous cap and lipid-rich necrotic core size in atherosclerotic carotid plaque: comparison of high-resolution, contrast-enhanced magnetic resonance imaging and histology. Circulation. 2005;112(22):3437–44.

51. Takaya N, Yuan C, Chu B, et al. Association between carotid plaque characteristics and subsequent ischemic cerebrovascular events: a prospective assessment with MRI—initial results. Stroke. 2006;37(3):818–23.

52. Laitinen I, Marjamaki P, Nagren K, et al. Uptake of inflammatory cell marker [11C]PK11195 into mouse atherosclerotic plaques. Eur J Nucl Med Mol Imaging. 2009;36(1):73–80.

53. Gaemperli O, Shalhoub J, Owen DR, et al. Imaging intraplaque inflammation in carotid atherosclerosis with 11C-PK11195 positron emission tomography/computed tomography. Eur Heart J. 2012;33(15):1902–10.

54. Fujimura Y, Hwang PM, Trout Iii H, et al. Increased peripheral benzodiazepine receptors in arterial plaque of patients with atherosclerosis: an autoradiographic study with [(3)H]PK 11195. Atherosclerosis. 2008;201(1):108–11.

55. Bird JL, Izquierdo-Garcia D, Davies JR, et al. Evaluation of translocator protein quantification as a tool for characterising macrophage burden in human carotid atherosclerosis. Atherosclerosis. 2010;210(2):388–91.

56. Dickens AM, Vainio S, Marjamaki P, et al. Detection of microglial activation in an acute model of neuroinflammation using PET and radiotracers 11C-(R)-PK11195 and 18F-GE-180. J Nucl Med. 2014;55(3):466–72.

57. Boutin H, Murray K, Pradillo J, et al. 18F-GE-180: a novel TSPO radiotracer compared to 11C-R-PK11195 in a preclinical model of stroke. Eur J Nucl Med Mol Imaging. 2015;42(3):503–11.

58. Kreisl WC, Jenko KJ, Hines CS, et al. A genetic polymorphism for translocator protein 18 kDa affects both in vitro and in vivo radioligand binding in human brain to this putative biomarker of neuroinflammation. J Cereb Blood Flow Metab. 2013;33(1):53–8.

59. Guo Q, Colasanti A, Owen DR, et al. Quantification of the specific translocator protein signal of 18F-PBR111 in healthy humans: a genetic polymorphism effect on in vivo binding. J Nucl Med. 2013;54(11):1915–23.

60. Lavisse S, Garcia-Lorenzo D, Peyronneau MA, et al. Optimized quantification of translocator protein radioligand (1)(8)F-DPA-714 uptake in the brain of genotyped healthy volunteers. J Nucl Med. 2015;56(7):1048–54.

61. Dalm VA, van Hagen PM, van Koetsveld PM, et al. Expression of somatostatin, cortistatin, and somatostatin receptors in human monocytes, macrophages, and dendritic cells. Am J Physiol Endocrinol Metab. 2003;285(2):E344–53.

62. Armani C, Catalani E, Balbarini A, Bagnoli P, Cervia D. Expression, pharmacology, and functional role of somatostatin receptor subtypes 1 and 2 in human macrophages. J Leukoc Biol. 2007;81(3):845–55.

63. Mojtahedi A, Alavi A, Thamake S, et al. Assessment of vulnerable atherosclerotic and fibrotic plaques in coronary arteries using (68)Ga-DOTATATE PET/CT. Am J Nucl Med Mol Imaging. 2015;5(1):65–71.

64. Li X, Samnick S, Lapa C, et al. 68Ga-DOTATATE PET/CT for the detection of inflammation of large arteries: correlation with18F-FDG, calcium burden and risk factors. EJNMMI Res. 2012;2(1):52.

65. Rominger A, Saam T, Vogl E, et al. In vivo imaging of macrophage activity in the coronary arteries using 68Ga-DOTATATE PET/CT: correlation with coronary calcium burden and risk factors. J Nucl Med. 2010;51(2):193–7.

66. Rinne P, Hellberg S, Kiugel M, et al. Comparison of somatostatin receptor 2-targeting PET tracers in the detection of mouse atherosclerotic plaques. Mol Imaging Biol. 2015. doi:10.1007/s11307-015-0873-1.

67. Pedersen SF, Sandholt BV, Keller SH, et al. 64Cu-DOTATATE PET/MRI for detection of activated macrophages in carotid atherosclerotic plaques: studies in patients undergoing endarterectomy. Arterioscler Thromb Vasc Biol. 2015;35(7):1696–703.

68. Malmberg C, Ripa RS, Johnbeck CB, et al. 64Cu-DOTATATE for noninvasive assessment of atherosclerosis in large arteries and its correlation with risk factors: head-to-head comparison with 68Ga-DOTATOC in 60 patients. J Nucl Med. 2015;56(12):1895–900.

69. Kelly-Arnold A, Maldonado N, Laudier D, Aikawa E, Cardoso L, Weinbaum S. Revised microcalcification hypothesis for fibrous

cap rupture in human coronary arteries. Proc Natl Acad Sci U S A. 2013;110(26):10741–6.

70. Chen W, Dilsizian V. Targeted PET/CT imaging of vulnerable atherosclerotic plaques: microcalcification with sodium fluoride and inflammation with fluorodeoxyglucose. Curr Cardiol Rep. 2013;15(6):364.

71. Demer LL, Tintut Y. Vascular calcification: pathobiology of a multifaceted disease. Circulation. 2008;117(22):2938–48.

72. Aikawa E, Nahrendorf M, Figueiredo JL, et al. Osteogenesis associates with inflammation in early-stage atherosclerosis evaluated by molecular imaging in vivo. Circulation. 2007;116(24): 2841–50.

73. Hawkins RA, Choi Y, Huang SC, et al. Evaluation of the skeletal kinetics of fluorine-18-fluoride ion with PET. J Nucl Med. 1992;33(5):633–42.

74.•• Irkle A, Vesey AT, Lewis DY, et al. Identifying active vascular microcalcification by (18)F-sodium fluoride positron emission tomography. Nat Commun. 2015;6:7495. **Study provides histological validation of NaF-PET signal in atheromatous plaques**.

75. Derlin T, Richter U, Bannas P, et al. Feasibility of 18F-sodium fluoride PET/CT for imaging of atherosclerotic plaque. J Nucl Med. 2010;51(6):862–5.

76. Morbelli S, Fiz F, Piccardo A, et al. Divergent determinants of 18F-NaF uptake and visible calcium deposition in large arteries: relationship with Framingham risk score. Int J Cardiovasc Imaging. 2014;30(2):439–47.

77. Fiz F, Morbelli S, Piccardo A, et al. 18F-NaF uptake by the atherosclerotic plaque at PET/CT imaging: inverse correlation between calcification density and mineral metabolic activity. J Nucl Med. 2015. doi:10.2967/jnumed.115.154229.

78. Derlin T, Wisotzki C, Richter U, et al. In vivo imaging of mineral deposition in carotid plaque using 18F-sodium fluoride PET/CT: correlation with atherogenic risk factors. J Nucl Med. 2011;52(3): 362–8.

79. Derlin T, Toth Z, Papp L, et al. Correlation of inflammation assessed by 18F-FDG PET, active mineral deposition assessed by 18F-fluoride PET, and vascular calcification in atherosclerotic plaque: a dual-tracer PET/CT study. J Nucl Med. 2011;52(7): 1020–7.

80. Dweck MR, Chow MW, Joshi NV, et al. Coronary arterial 18F-sodium fluoride uptake: a novel marker of plaque biology. J Am Coll Cardiol. 2012;59(17):1539–48.

81.•• Joshi NV, Vesey AT, Williams MC, et al. 18F-fluoride positron emission tomography for identification of ruptured and high-risk coronary atherosclerotic plaques: a prospective clinical trial. Lancet. 2014;383(9918):705–13. **Key paper demonstrating utility of NaF-PET for detection of vulnerable coronary atherosclerotic plaques**.

82. Quirce R, Martinez-Rodriguez I, De Arcocha TM, et al. Contribution of 18F-sodium fluoride PET/CT to the study of the carotid atheroma calcification. Rev Esp Med Nucl Imagen Mol. 2013;32(1):22–5.

83. Rubeaux M, Joshi NV, Dweck MR, et al. Motion correction of 18F-NaF PET for imaging coronary atherosclerotic plaques. J Nucl Med. 2016;57(1):54–9.

84. Zemplenyi T, Crawford DW, Cole MA. Adaptation to arterial wall hypoxia demonstrated in vivo with oxygen microcathodes. Atherosclerosis. 1989;76(2–3):173–9.

85. Leppanen O, Bjornheden T, Evaldsson M, Boren J, Wiklund O, Levin M. ATP depletion in macrophages in the core of advanced rabbit atherosclerotic plaques in vivo. Atherosclerosis. 2006;188(2):323–30.

86. Tawakol A, Singh P, Mojena M, et al. HIF-1alpha and PFKFB3 mediate a tight relationship between proinflammatory activation and anaerobic metabolism in atherosclerotic macrophages. Arterioscler Thromb Vasc Biol. 2015;35(6):1463–71.

87. Lee SJ, Thien Quach CH, Jung KH, et al. Oxidized low-density lipoprotein stimulates macrophage 18F-FDG uptake via hypoxia-inducible factor-1alpha activation through Nox2-dependent reactive oxygen species generation. J Nucl Med. 2014;55(10):1699–705.

88. Mateo J, Izquierdo-Garcia D, Badimon JJ, Fayad ZA, Fuster V. Noninvasive assessment of hypoxia in rabbit advanced atherosclerosis using (1)(8)F-fluoromisonidazole positron emission tomographic imaging. Circ Cardiovasc Imaging. 2014;7(2):312–20.

89. Joshi FR, Manavaki R, Fryer TD, et al. Imaging of hypoxia and inflammation in carotid atherosclerosis with 18F-fluoromisonidazole and 18F-fluorodeoxyglucose positron emission tomography. Circulation. 2013;128 Suppl 22, A14673.

90. van der Valk FM, Sluimer JC, Voo SA, et al. In vivo imaging of hypoxia in atherosclerotic plaques in humans. JACC Cardiovasc Imaging. 2015;8(11):1340–1.

91. Hoffman EJ, Huang SC, Phelps ME. Quantitation in positron emission computed tomography: 1. Effect of object size. J Comput Assist Tomogr. 1979;3(3):299–308.

92. Rousset OG, Ma Y, Evans AC. Correction for partial volume effects in PET: principle and validation. J Nucl Med. 1998;39(5):904–11.

93. Izquierdo-Garcia D, Davies JR, Graves MJ, et al. Comparison of methods for magnetic resonance-guided [18-F]fluorodeoxyglucose positron emission tomography in human carotid arteries: reproducibility, partial volume correction, and correlation between methods. Stroke. 2009;40(1):86–93.

94. Huet P, Burg S, Le Guludec D, Hyafil F, Buvat I. Variability and uncertainty of FDG PET imaging protocols for assessing inflammation in atherosclerosis: suggestions for improvement. J Nucl Med. 2015. doi:10.2967/jnumed.114.142596.

95. Niccoli Asabella A, Ciccone MM, Cortese F, et al. Higher reliability of 18F-FDG target background ratio compared to standardized uptake value in vulnerable carotid plaque detection: a pilot study. Ann Nucl Med. 2014;28(6):571–9.

96. Oh M, Kim JY, Shin KH, et al. Imaging atherosclerosis in the carotid arteries with F-18-Fluoro-2-deoxy-D-glucose positron emission tomography: effect of imaging time after injection on quantitative measurement. Nucl Med Mol Imaging. 2010;44(4): 261–6.

97. Derlin T, Habermann CR, Hahne JD, et al. Quantification of [18F]-FDG uptake in atherosclerotic plaque: impact of renal function. Ann Nucl Med. 2011;25(8):586–91.

98. Bucerius J, Hyafil F, Verberne HJ, et al. Position paper of the Cardiovascular Committee of the European Association of Nuclear Medicine (EANM) on PET imaging of atherosclerosis. Eur J Nucl Med Mol Imaging. 2015. doi:10.1007/s00259-015-3259-3.

99. Tahara N, Kai H, Ishibashi M, et al. Simvastatin attenuates plaque inflammation: evaluation by fluorodeoxyglucose positron emission tomography. J Am Coll Cardiol. 2006;48(9): 1825–31.

100. Tawakol A, Fayad ZA, Mogg R, et al. Intensification of statin therapy results in a rapid reduction in atherosclerotic inflammation: results of a multicenter fluorodeoxyglucose-positron emission tomography/computed tomography feasibility study. J Am Coll Cardiol. 2013;62(10):909–17.

101. Wu YW, Kao HL, Huang CL, et al. The effects of 3-month atorvastatin therapy on arterial inflammation, calcification, abdominal adipose tissue and circulating biomarkers. Eur J Nucl Med Mol Imaging. 2012;39(3):399–407.

102. Fayad ZA, Mani V, Woodward M, et al. Safety and efficacy of dalcetrapib on atherosclerotic disease using novel non-invasive multimodality imaging (dal-PLAQUE): a randomised clinical trial. Lancet. 2011;378(9802):1547–59.

103. Schwartz GG, Olsson AG, Abt M, et al. Effects of dalcetrapib in patients with a recent acute coronary syndrome. N Engl J Med. 2012;367(22):2089–99.

104. Emami H, Vucic E, Subramanian S, et al. The effect of BMS-582949, a P38 mitogen-activated protein kinase (P38 MAPK) inhibitor on arterial inflammation: a multicenter FDG-PET trial. Atherosclerosis. 2015;240(2):490–6.

105. Calcagno C, Ramachandran S, Izquierdo-Garcia D, et al. The complementary roles of dynamic contrast-enhanced MRI and 18F-fluorodeoxyglucose PET/CT for imaging of carotid atherosclerosis. Eur J Nucl Med Mol Imaging. 2013;40(12):1884–93.

106. Saito H, Kuroda S, Hirata K, et al. Validity of dual MRI and F-FDG PET imaging in predicting vulnerable and inflamed carotid plaque. Cerebrovasc Dis. 2013;35(4):370–7.

107. Ripa RS, Knudsen A, Hag AM, et al. Feasibility of simultaneous PET/MR of the carotid artery: first clinical experience and comparison to PET/CT. Am J Nucl Med Mol Imaging. 2013;3(4):361–71.

108. Hyafil F, Schindler A, Sepp D, et al. High-risk plaque features can be detected in non-stenotic carotid plaques of patients with ischaemic stroke classified as cryptogenic using combined F-FDG PET/MR imaging. Eur J Nucl Med Mol Imaging. 2015. doi:10.1007/s00259-015-3201-8.